Analysis of short-period internal waves using wave-induced surface displacement: A three-dimensional model approach in Algeciras Bay and the Strait of Gibraltar

Óscar Álvarez,[1] Carlos J. González,[1] Rafael Mañanes,[1] Laura López,[1] Miguel Bruno,[1] Alfredo Izquierdo,[2] Jesús Gómez-Enri,[1] and Manuel Forero[1]

Received 23 June 2011; revised 14 October 2011; accepted 21 October 2011; published 22 December 2011.

[1] A three-dimensional, nonlinear, high-resolution, sigma coordinate, hydrodynamic model was applied to study the sea surface manifestation of short-period internal waves measured in Algeciras Bay and the Strait of Gibraltar. Model results reproduce the tidally induced generation of the internal bore over the Camarinal Sill and its disintegration into wave trains as it moves eastward. While propagating along the Strait of Gibraltar toward the Mediterranean Sea, the wave trains partly penetrate into Algeciras Bay, with typical oscillation periods of 20 and 40 min. The modeled wave-induced surface train structures are compared with satellite images and in situ observational data obtained from two pressure sensors located inside the bay. Results demonstrate that wave-induced sea surface displacements are indicators of the presence of internal waves and may be used in the context of the internal wave analysis when surface oscillations are captured with sufficient precision.

Citation: Álvarez, Ó., C. J. González, R. Mañanes, L. López, M. Bruno, A. Izquierdo, J. Gómez-Enri, and M. Forero (2011), Analysis of short-period internal waves using wave-induced surface displacement: A three-dimensional model approach in Algeciras Bay and the Strait of Gibraltar, *J. Geophys. Res.*, *116*, C12033, doi:10.1029/2011JC007393.

1. Introduction

[2] The displacement of the sea surface is one of the physical manifestations of the internal wave phenomena. However, on the grounds that the small amplitude of that displacement is very small in comparison to those of the isopycnal surfaces around the pycnocline, surface displacement is usually disregarded in the majority of studies on internal waves, which invoke the so-called "rigid lid" assumption. The paper is aimed to investigate the sea surface displacement induced by internal waves in Algeciras Bay and the Strait of Gibraltar.

[3] Algeciras Bay is situated near latitude 36.2°N, at the northeastern end of the Strait of Gibraltar (Figure 1). Here the Atlantic waters flow into the Mediterranean Sea as a surface current, while the denser Mediterranean outflow waters flow in the opposite direction at depth. Superimposed on this quasi-steady two-layer water exchange there are a predominantly mesotidal and semidiurnal tide dynamics that have been extensively described [*Candela et al.*, 1990; *Mañanes et al.*, 1998; *Tejedor et al.*, 1999; *Parrilla et al.*, 2002; *Sánchez-Román et al.*, 2008]. The interaction of the barotropic tide with the abrupt topography of the Camarinal Sill in the presence of such strong stratification generates internal waves, which propagate mainly toward the Mediterranean Sea. These internal disturbances decompose into wave trains during the propagation and their structure has also been described in extensively [*Armi and Farmer*, 1988; *Tsimplis*, 2000; *Izquierdo et al.*, 2001; *Bruno et al.*, 2002].

[4] At present, a hierarchy of numerical models has been developed to describe the hydrodynamics of the strait. These are based on two-dimensional depth-integrated schemes [*Sánchez and Pascual*, 1989; *Tejedor et al.*, 1998], two-layer models [*Izquierdo et al.*, 2001], three-dimensional, hydrostatic models [*Wang*, 1993; *Sannino et al.*, 2007], two-dimensional (in a vertical plane), nonhydrostatic models [*Morozov et al.*, 2002; *Vázquez et al.*, 2006] and three-dimensional nonhydrostatic models [*Vlasenko et al.*, 2009]. The numerical model by *Vlasenko et al.* [2009] reproduces the propagation of wavefronts from the generation of internal waves included as a forcing in the initial conditions, whereas the two-dimensional model of *Vázquez et al.* [2006] simulates the processes of generation and disintegration of internal wavefronts from the Camarinal Sill considering the rigid lid approximation.

[5] Despite the large amount of data collected in the Strait of Gibraltar, there is a lack of field measurements and numerical results in Algeciras Bay. For these reasons the dynamic processes of Algeciras Bay are not yet well known. As evidence of this, although there are data from the analysis of tidal elevation at some points within the bay [*García-Lafuente*, 1986; *Candela*, 1990; *Tsimplis et al.*, 1995; *Pairaud et al.*, 2008], from the reported presence of internal waves fronts near the mouth of Algeciras Bay [*Watson and Robinson*,

[1]Department of Applied Physics, University of Cadiz, Puerto Real, Spain.
[2]Department of Ocean in the Earth System, Max Planck Institute for Meteorology, Hamburg, Germany.

0148-0227/11/2011JC007393

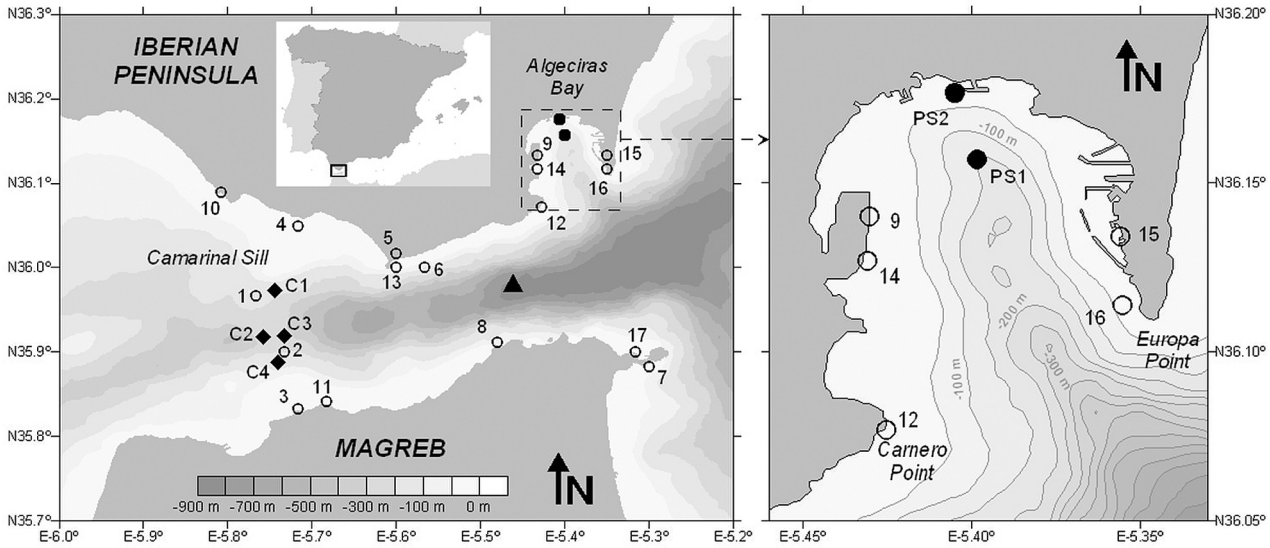

Figure 1. (left) Bathymetry of the Strait of Gibraltar and (right) detail of Algeciras Bay. The locations of the experimental stations referred to in section 3 (open circles 1–17, surface elevation; diamonds C1–C4, velocity profiles; solid circles PS1 and PS2, pressure sensors within Algeciras Bay) and the control point on the eastern side of the strait (solid triangle) are also shown superimposed on the bathymetry.

1990, 1991], and from experimental records on the oceanographic characteristics of the bay (see Environmental Quality Plan for the Campo de Gibraltar, 2004, available at www2.uca.es/grup-invest/plan-campodegibraltar/), the most recent specific study conducted in this geographic context is dated 1924 [*De Buen*, 1924].

[6] The bay is deep, with maximum depths of more than 500 m in a broad central canyon that characterizes the bathymetry, running longitudinally until it reaches the Strait of Gibraltar. Since Algeciras Bay opens into the strait, the propagation of internal waves into the bay is potentially one of the hydrodynamic processes affecting the mean values and variability of several significant oceanographic features. However, the only evidence of this process to date consists in some remote sensing satellite images [see, e.g., *Global Ocean Associates*, 2002].

[7] In this paper, the generation of short-period internal wave trains in the Strait of Gibraltar and their propagation into Algeciras Bay are studied by analyzing the wave induced sea surface displacement, by use of a three-dimensional, semi-implicit model, in conjunction with observational data. The paper is organized as follows. Section 2 describes the characteristics of the numerical model. In section 3 we present the model results; here, we make a comparison between the observed and modeled values of the M_2 tidal characteristics, and analyze and compare the propagation of short-period internal waves with the available experimental information. Final concluding remarks complete the paper in section 4.

2. Model

[8] A three-dimensional, nonlinear, high-resolution, baroclinic, free-surface, hydrodynamic model was developed on the basis of the numerical resolution of the 3-D primitive hydrostatic equations, in sigma coordinates, as described by *Mellor* [1996]. Equations solve the momentum balance, the conservation of mass, temperature and salinity, and the UNESCO equation of state for the density. The coefficients of vertical viscosity and diffusion are calculated by means of a *Mellor and Yamada* [1982] second-order closure scheme.

[9] In order to achieve an accurate representation of the elevation fields, the model solves simultaneously the 2-D (depth-averaged) hydrodynamic equations coupled to the 3-D scheme by means of splitting techniques. The solution of the 2-D equations provides the free-surface baroclinic elevation and the mean depth-averaged velocity profiles with the high accuracy associated with depth-averaged models. In correspondence, the 2-D terms of advection, horizontal and vertical diffusivity, and baroclinic pressure gradient are calculated by the three-dimensional equations by integrating over the depth. The bottom stress is solved by matching the numerical solution to the 'law of the wall' applied to the first grid points nearest the bottom. A bottom roughness parameter z_0 = 0.1 cm was specified on the basis of a reference height of 1 m above the bottom for a drag coefficient C_D = 0.003. Equations of motion were completed with a horizontal eddy diffusion term acting on the velocity. Here, the horizontal eddy viscosity coefficient, K_0 = 0.05 m^2 s^{-1}, was chosen because it is the smallest value capable of suppressing nonphysical disturbances in the model solution.

[10] The horizontal structure of equations were integrated on an Arakawa-C staggered grid by a semi-implicit Crank-Nicolson scheme, using the *Peaceman and Rachford* [1955] splitting-up method as in the UCA2D model [*Álvarez et al.*, 1999], while an implicit scheme was used for the vertical diffusion terms in the 3-D equations [*Richtmyer and Morton*, 1967]. This scheme is conservative and unconditionally stable [*Marchuk*, 1980], and provides high numerical stability and computational efficiency. This characteristic is particularly needed when short-period waves and high nonlinear contributions are present, since it allows for the use of fine

Table 1. Model Validation for the M_2 Tidal Elevation[a]

Source	ID	Station		Amplitude[b] (cm)		Phase[c] (deg Greenwich)	
		Longitude (deg E)	Latitude (deg N)	Observed	Predicted	Observed	Predicted
Candela [1990]	1	−5.7667	35.9667	60.1	56.2	51.8	55.4
	2	−5.7333	35.9000	54.0	55.1	61.8	57.2
	3	−5.7167	35.8333	57.1	56.5	66.8	66.0
	4	−5.7167	36.0500	52.3	53.4	47.6	48.5
	5	−5.6000	36.0167	41.2	43.6	41.2	43.0
	6	−5.5667	36.0000	44.4	42.2	47.6	45.4
	7	−5.3000	35.8833	29.7	29.6	50.3	52.2
	8	−5.4800	35.9117	36.4	37.8	46.5	51.2
	9	−5.4333	36.1333	31.0	32.3	48.0	47.3
García-Lafuente [1986]	10	−5.8083	36.0900	64.9	63.6	49.0	52.1
	11	−5.6833	35.8417	51.8	47.9	69.0	58.5
	12	−5.4283	36.0717	31.1	33.6	47.5	44.6
García and Molinero [2006]	13	−5.6000	36.0000	40.2	44.1	40.5	43.7
Pairaud et al. [2008]	14	−5.4331	36.1169	32.0	32.3	48.0	47.0
Tsimplis et al. [1995]	15	−5.3500	36.1333	29.8	33.0	46.0	48.5
WOCE[d] (NOAA)	16	−5.3500	36.1167	31.8	33.0	50.0	47.5
	17	−5.3167	35.9000	30.3	31.7	49.8	52.2
Own data	PS1	−5.3983	36.1572	30.0	32.2	50.1	48.5
	PS2	−5.4058	36.1773	32.0	32.2	45.9	48.9

[a]Observed and predicted M_2 amplitudes and phases of free-surface elevation for 17 stations reported in the literature and the two pressure sensors inside Algeciras Bay (see Figure 1).
[b]RMS error = 2.2 cm.
[c]RMS error = 3.5°.
[d]WOCE, World Ocean Circulation Experiment 1990–2002; see http://woce.nodc.noaa.gov.

horizontal and vertical resolutions without numerical energy losses and the requirement of shortened time steps.

[11] The calculation grid domain covered the Strait of Gibraltar and the western zone of the Alboran Sea (Figure 1), with a horizontal resolution of 100 m and 50 sigma levels in the vertical direction. The bathymetry was obtained from nautical charts published by the Spanish Navy Hydrographic Institute (IHM) and the British Admiralty. The time step for integration was 2 s, which ensures the stability of the numerical solution.

[12] A free slip condition was set at the coastal boundaries. At the open boundaries, a radiation condition in the 2-D equations was imposed [*Flather and Heaps*, 1975], so that the nonphysical disturbances are propagated away from the model domain. This condition is written in terms of the deviations of tidal elevation and the mean depth-averaged velocity from their reference values. In the 3-D equations, the spatial variability of currents related to its mean depth-averaged value normal to the open boundaries was implemented through the well-known Sommerfeld radiation condition in the form of *Orlanski* [1976]. In order to avoid short-period wave reflections at the open boundaries, the equations adjacent to these boundaries were supplemented with artificial smoothing terms, defined as a numerical filter acting on the tidal velocity and elevation.

[13] The model was forced at the western and eastern open boundaries with a M_2 tidal elevation and velocity and a steady baroclinic exchange. The reference amplitudes and phases of elevation and velocity of this boundary condition were inferred from the previous studies by *Tejedor et al.* [1998], *Bruno et al.* [2000], and *Izquierdo et al.* [2001], by interpolation/extrapolation techniques and taking into account basic flow-conservation laws.

[14] The initial vertical profiles of temperature and salinity for the whole domain were implemented according to the empirical data collected during the experiment "Strait 94–96," which show the general pattern for the strait to be constituted by two main density-defined water layers (upper Atlantic and lower Mediterranean) together with a transition layer between them at a depth of ~100 m. A initial homogeneous mean field was implemented, also taking into consideration the results given by *Bruno et al.* [2000], *Tsimplis* [2000], and *Izquierdo et al.* [2001]. At the open boundaries, the temperature and salinity conditions are prescribed by means of a standard upstream advection scheme.

[15] The model results analyzed in section 3 correspond to the last 10 M_2 tidal cycles simulated, once a steady time periodic solution was achieved. Once the series were obtained, the output data were processed by techniques of harmonic [*Foreman and Henry*, 1989] and spectral [*Godin*, 1972] analysis to obtain the tidal characteristics and the presence of short-period waves on the free surface, generated by internal wavefronts.

3. Results

3.1. Experimental Comparison of M_2 Tidal Model Results

[16] A total of 23 locations, shown in Figure 1, have been used in order to make a comparison between the observed values of the M_2 tidal characteristics and those modeled. Table 1 shows the comparison for M_2 tidal elevation amplitude and phase in 19 sites. Mean differences between the predicted and observed values are smaller than 2.5 cm for the tidal amplitude and 3.6° for the phase. More specifically, in the area of Algeciras Bay model results are found to be in clear agreement with the experimental results, and show maximum differences over the whole domain of 2 cm in the amplitude and 3° in the phase. Figure 2 shows the observed and calculated M_2 current ellipse parameters. Here, the quantitative similarity of the data is notable. Namely, the RMS error for the semimajor axes is 20.2 cm s^{-1} for the

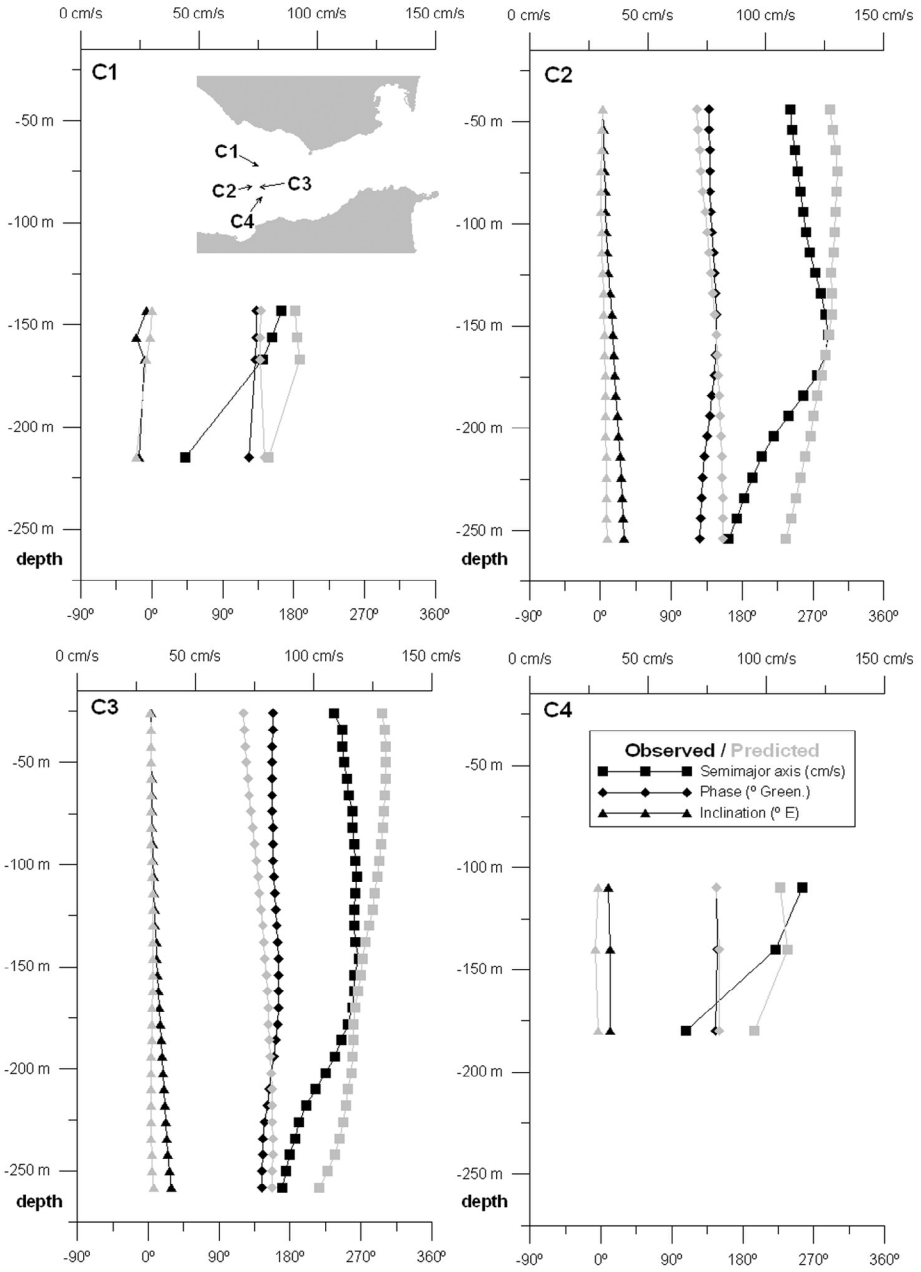

Figure 2. Comparison between observed (black) and predicted (gray) vertical profiles of the M_2 current velocity ellipses' parameters for different experimental stations C1 and C4 [*Candela*, 1990], C2 [*Bruno et al.*, 2000], and C3 (modified from *Tsimplis* [2000]), showing the ellipses' semimajor axis (squares), phase (diamonds), and inclination (triangles).

station C1, 14.5 cm s^{-1} for C2, 13.0 cm s^{-1} for C3, and 17.8 cm s^{-1} for C4. These values are one order of magnitude less than the mean amplitude of M_2 currents, and the inclination of the semimajor axis and the phase of maximum velocity are almost coincident in all cases.

[17] The modeling results for the spatial distribution of the amplitudes and phases of the M_2 tidal elevation is shown in Figure 3. The M_2 tidal amplitude shows a smooth variation between the extremes of the domain, ranging from 65 cm at the western limit to 30 cm at the eastern boundary, while the phases, showing small variations in consonance with the measurements reported by *Candela* [1990], give evidence of slight propagation southwestward, in accordance with the numerical results of *Tejedor et al.* [1998] and *Sannino et al.* [2007]. In Algeciras Bay, the amplitude of the co-oscillating M_2 tide remains around 33 cm and the cotidal lines indicate a northward propagation and a diffraction process on the headland constituted by the Rock of Gibraltar.

3.2. Simulation of Internal Wave Generation at the Camarinal Sill and Its Manifestation on Free-Surface Elevation

[18] Figure 4 shows the predicted evolution of the free-surface elevation and vertical component of current velocity

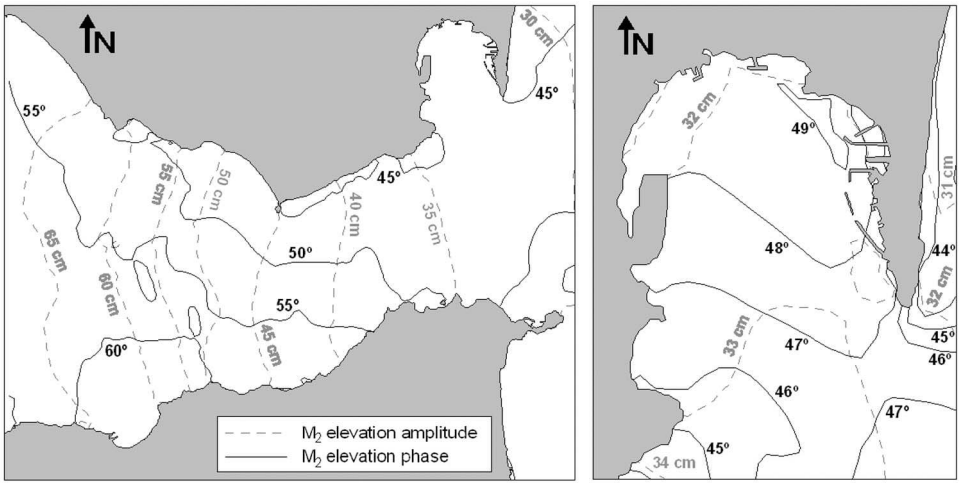

Figure 3. Predicted tidal charts for the M_2 elevation amplitude (dashed lines) and phase (solid lines). (left) Strait of Gibraltar. (right) Detail of Algeciras Bay.

during one M_2 tidal cycle at a control point at the eastern side of the Strait of Gibraltar (shown in Figure 1). The most remarkable feature is a high-frequency perturbation in the free-surface elevation generated around 4 h after the high tide (Figure 4a). This signal is most perceptible when the series is submitted to a process of high-pass Fourier filtering to eliminate periods longer than 1 h. Perturbations with amplitudes close to 4 cm can be appreciated. These oscillations are accompanied by variations in the vertical component of current velocity at a depth of 50 m, representative of the mean interface depth (Figure 4b), with amplitudes of up to 5 cm s^{-1}. The spectral analyses of the filtered series show that these oscillations are associated with peaks between 20 and 40 min.

[19] Similar short-period oscillations also appear in the density field along a longitudinal transect of the strait (Figure 5a). Note that, as expected, the sea surface displacement is in opposite phase to the isopycnal displacement

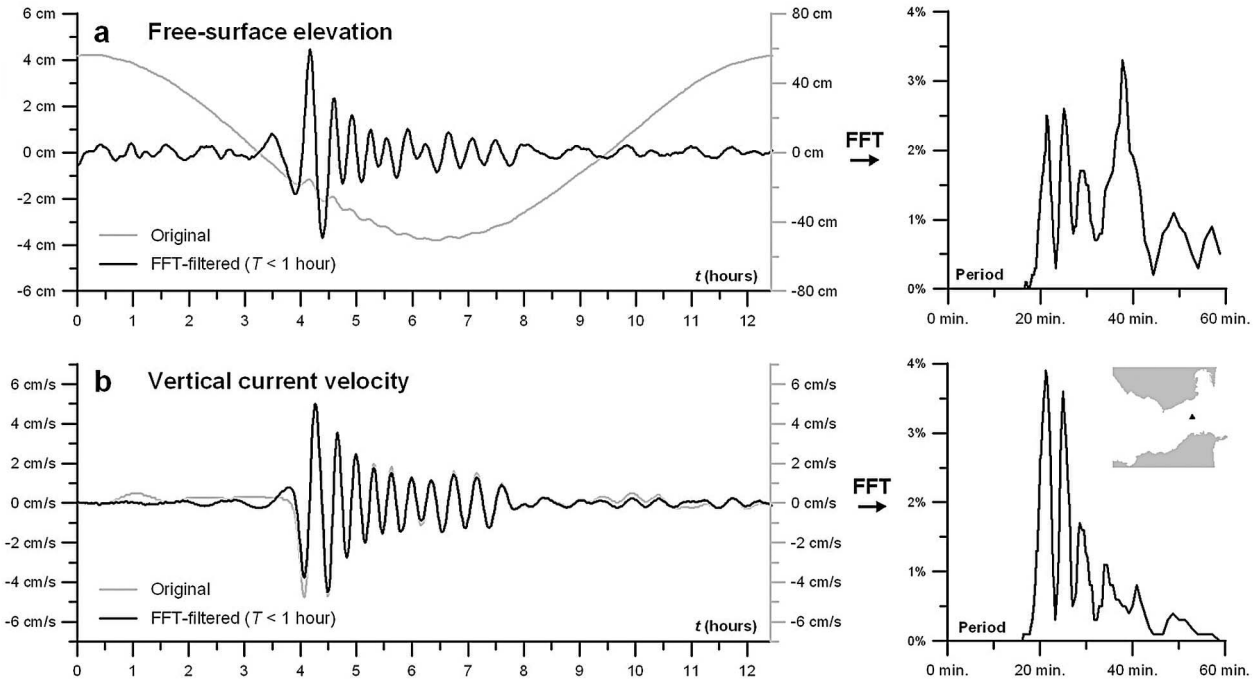

Figure 4. (a) Original (gray line) and FFT-filtered (periods longer than 1 h removed; black line) time series of predicted free-surface elevation during one M_2 cycle at a control point of the Strait of Gibraltar together with the distribution of spectral density (in percentage) from the filtered series. (b) Same as Figure 4a for the vertical component of current velocity (w) at a depth of 50 m.

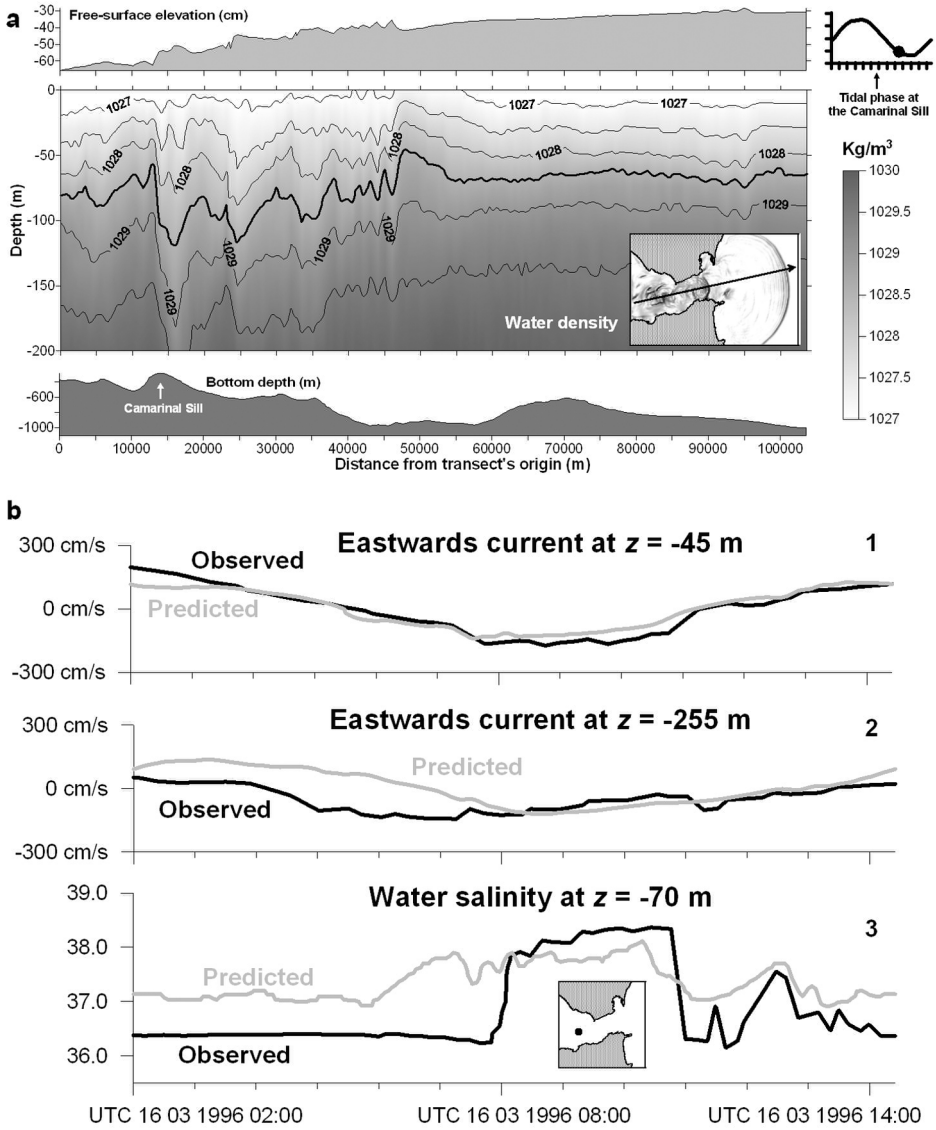

Figure 5. (a) Section of predicted water density (until 200 m depth) through the main longitudinal axis of the Strait of Gibraltar at a selected time together with the related free-surface elevation (up) and bottom topography (down). (b) Experimental (black lines) and modeled (gray lines) time series of eastward current at depths of 45 m and 255 m, as well as water salinity at a depth of 70 m, during one M_2 tidal cycle at a point over Camarinal Sill (corresponding to the C2 station in Figure 1); the experimental series were collected during the experiment "Strait 94–96" [*Vázquez et al.*, 2008] in situation of mean tide.

and a crest/trough in the isopycnal corresponds to a trough/crest in the sea surface. Here, ~6 h after the release of the internal bore generated at the Camarinal Sill, short-wavelength oscillations of the isopycnals resulting from the disintegration of the internal bore can be observed, in accordance with the descriptions by *Gerkema* [1994], *Tsimplis* [2000], and *Bruno et al.* [2002]. These isopycnal oscillations are clearly correlated with free-surface displacements, as can be appreciated in Figure 5a. Complementarily, Figure 5b shows the observed and modeled time variation of salinity at a depth of 70 m in a location over Camarinal Sill (corresponding to the C2 station in Figures 1 and 2) during a specific period covering the internal wave advance; the experimental series correspond to the experiment "Strait 94–96" [*Vázquez et al.*, 2008]. Salinity values increase suddenly (from 36.5 to 38.3 in the experimental record, and from 37.0 to 38.1 in the modeled series) at the time of the hydraulic jump when the Mediterranean water moves upward, coinciding with maximum westward currents (Figure 5b); the values are then restored during the turning tide. A secondary, smaller increase in salinity can be observed about 1.5 h later, in both time series: measured (from 36.5 to 37.5) and modeled (from 37.0 to 37.5). The results also show how the perturbed density field depicts a rank-ordered wave train, consonant with the patterns described by *Vázquez et al.* [2006].

[20] Figure 6a shows a sequence of the predicted elevation fields of the free surface and the vertical component of the

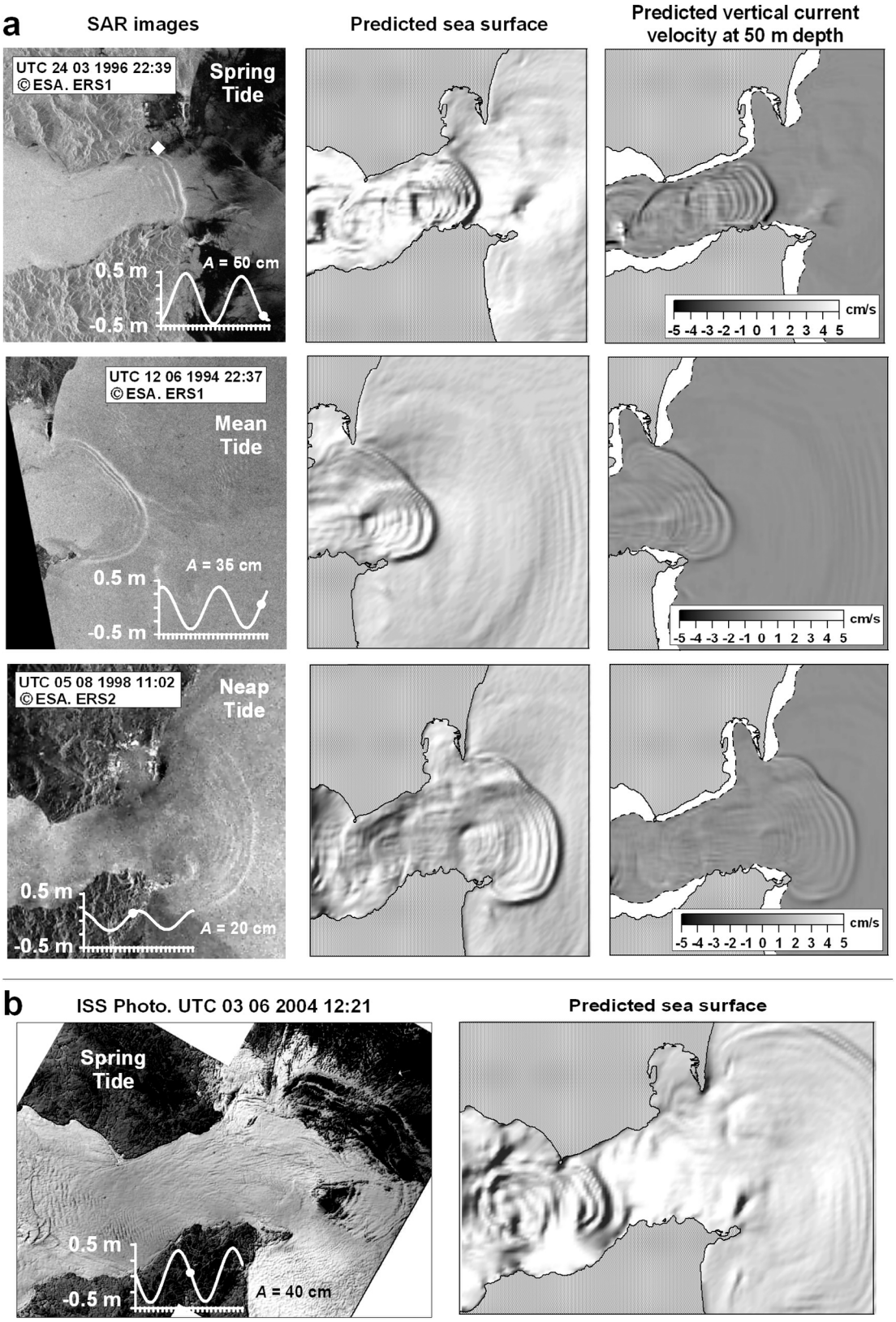

Figure 6. Comparison between images from space and model results for four different tidal stages, indicated by the white plots together with the elevation amplitude values at Carnero Point (white diamond) and increasing downward. (a) SAR images (courtesy of ESA), predicted free-surface elevation, and predicted vertical current velocity at 50 m depth. (b) Composition of the ISS009-E-9952 and ISS009-E-9954 photos taken from the International Space Station (courtesy of NASA) and predicted free-surface elevation.

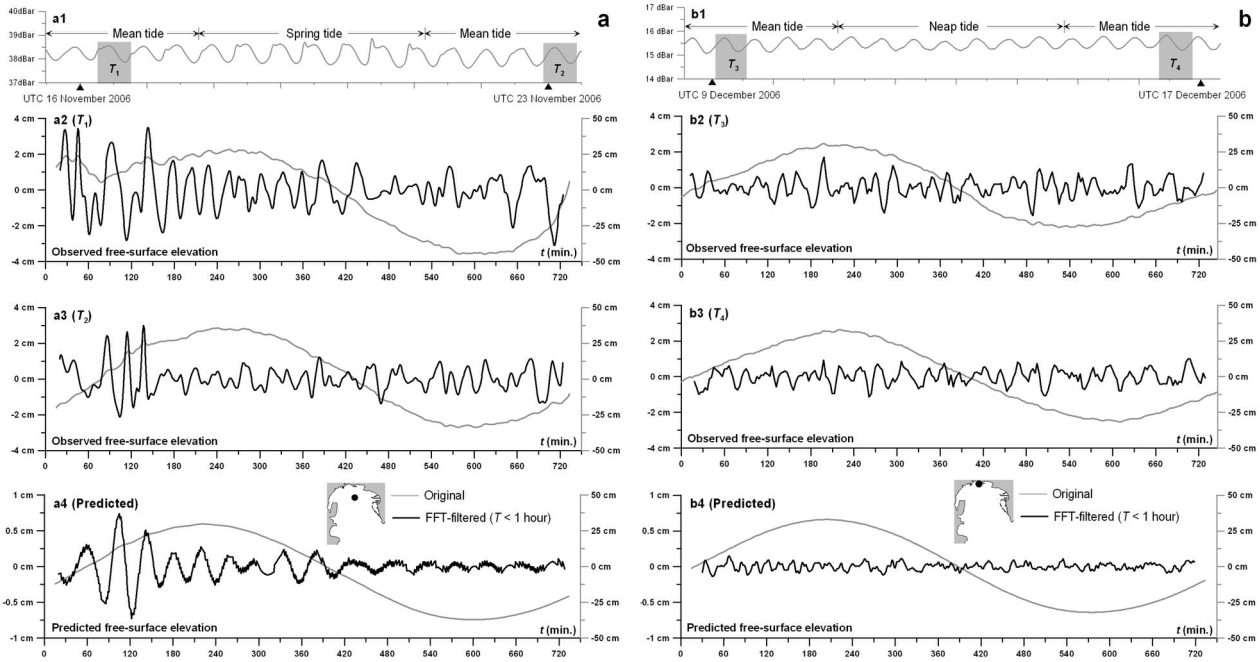

Figure 7. (a) Evidence of the effects of the internal wave on the free surface of water from the pressure sensor at the upper central canyon of Algeciras Bay (PS1). From top to bottom: original series of instrument's depth; detail of original (gray line) and FFT-filtered (periods longer than 1 h removed; black line) experimental series of free-surface elevation during two M_2 tidal cycles in mean tide episodes; and corresponding predicted series at the same location. (b) The same for the station near the northern coast of the bay (PS2).

current velocity at a depth of 50 m, together with three SAR images from the ERS-1 and ERS-2 satellites (ESA), at different moments of the tidal cycle. From the analysis of Figure 6a, a considerable correspondence is found between model fields and the images from space, despite the spring or neap tide episodes corresponding to some of the satellite images, which would imply different conditions with respect to the mean tide situation contemplated by the model. A detailed analysis of these images reveals the generation and release of one internal bore for each M_2 cycle, which disintegrates into a wave train with 7 to 10 wavefronts during its propagation toward the Mediterranean Sea. Model results show amplitudes of about 4 cm for the elevation, 5 cm s^{-1} for the vertical velocity, and 40 to 65 m for the isopycnals, with oscillation periods ranging from 20 to 40 min, wavelengths of 1.8 to 2.1 km and propagation velocity of about 5 km h^{-1}, in good agreement with the values described by *Gerkema* [1994], *Vázquez et al.* [2006], and *Sánchez Garrido et al.* [2008]. Model results similarly show how the wave train, in its transit through the strait, penetrates into Algeciras Bay when it reaches its mouth. This behavior is also observed in the photo taken from the International Space Station (ISS) in June 2004 (Figure 6b).

3.3. Propagation of Internal Wave Trains Into Algeciras Bay

[21] To evaluate the presence of short-period internal wave trains in Algeciras Bay, the experimental data series acquired by two pressure sensors at depths of 40 and 16 m and situated at the control points PS1 and PS2, respectively, were analyzed. These sensors made recording over periods of 1 month during November 2006 (PS1) and December 2006 (PS2) with sampling intervals of 1 and 3 min, respectively. Predicted and observational results are shown in Figures 7 and 8.

[22] Figure 7a shows the temporal evolution of the elevation of the free surface inferred from the pressure sensor at the control location PS1, during the course of 15 wave cycles. A simple visual inspection of the observed data reveals not only that the amplitude and phase of the measured tidal oscillations are close to those of the modeled M_2 tide, but also that short-period perturbations are present, superimposed on the tide in the original series, close to high tide. The intensity of the perturbations is unequal, with values appreciably higher in episodes of spring tides compared with the same behavior in other stages of the spring-neap cycle, plausibly correlated with the different values of the Froude number for supercritical flows [*Izquierdo et al.*, 2001]. This evidence, related to the presence of these waves, becomes clearer when the series is submitted to a high-pass filtering in order to eliminate periods longer than 1 h. In fact, when these results for the observed amplitude during two tidal cycles, separated in time by 7 days, are compared with the equivalent amplitudes of the predicted M_2 tidal constituent (see Figure 7a), it becomes evident that there is a qualitatively and quantitatively analogous oscillation, situated in the same phase of the wave as that obtained experimentally. By monitoring the evolution of the spatial propagation of the wavefronts generated numerically, these waves can be associated with the perturbation of the free

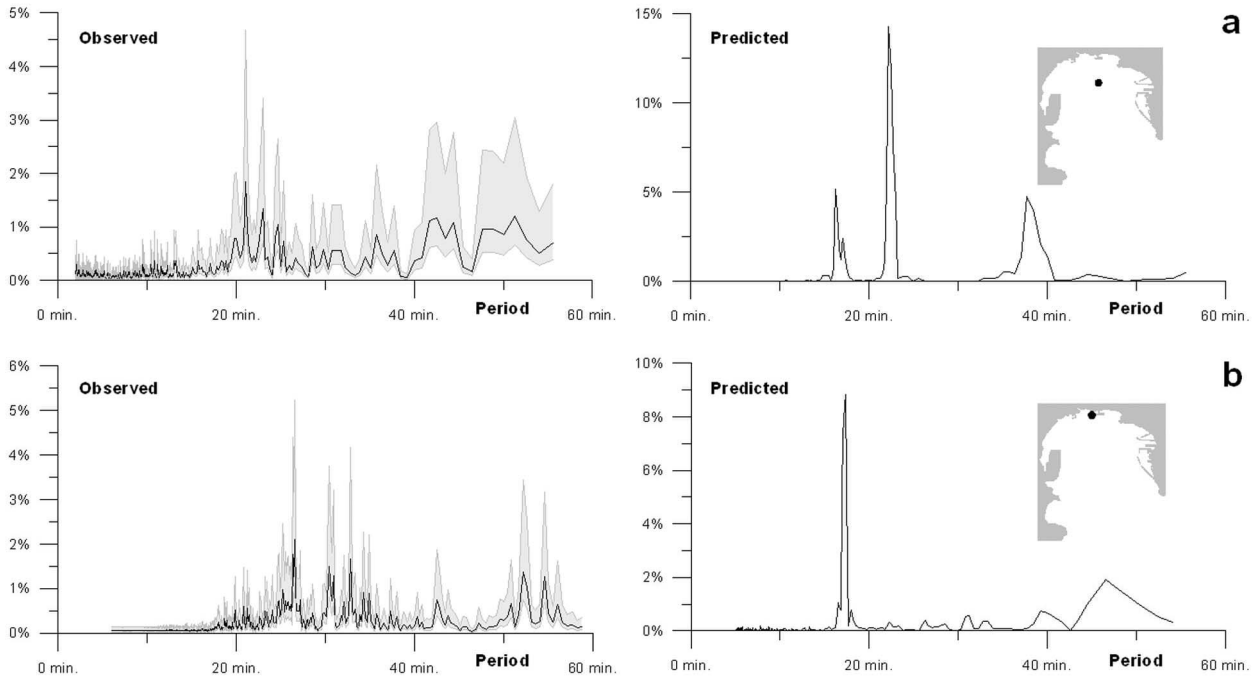

Figure 8. (a) Observed (95% confidence intervals shaded in gray) and predicted distributions of spectral density (in percentage) from the series of free-surface elevation (periods longer than 1 h removed) from the station at the upper central canyon of Algeciras Bay (PS1). (b) Same as Figure 8a but for the station near the northern coast of the bay (PS2).

surface produced by the internal wave train generated in the strait. Figure 7b shows the corresponding analyses for the pressure sensor at the control location PS2. The short-period oscillations in the free surface have lower amplitudes, both in observed and predicted series, owing to the weakening of the internal waves as they penetrate into the bay, and because the strong vertical stratification does not appear in the well-mixed shallower nearshore areas.

[23] However, owing to the apparent variability in the amplitude of the short-period waves observed in different tidal cycles, a merely quantitative and isolated comparison of the amplitudes between the observed and calculated data could be an insufficient indicator for their characterization. Hence, additional analyses are necessary.

[24] Figure 8 shows the spectral density distribution of the observed and predicted free-surface elevation time series data were filtered to remove periods longer than 1 h at the two mooring locations in the bay. At both points, the experimental data present analogous spectral distributions. Specifically, a main peak at periods close to 20 min for both locations is the principal characteristic of the spectra, both in the predicted series and in the observed data. In numerical terms, the main energy peak of the experimental spectrum at the PS1 station corresponds to a period of 22 min, while for the PS2 station such peak occurs at a period of 26 min. Similarly, three secondary peaks for periods of around 18, 25, and 40 min can be noted at the predicted PS1 spectral distribution. Plausibly, the relatively higher predicted densities for all these peaks are due to the clearer signal of the modeled series, which avoids the subsequent spreading of energy over the different frequency bands that occurs in the experimental analyses.

[25] The frequency range where the significant peaks appear also shows the persistent presence of very small-amplitude periodic oscillations in the wave train propagation area, behind the internal tide oscillation, evident in both the calculated and observed data. Such oscillations, apparently not directly originated by the wave train, are plausibly related to the resonant period for Algeciras Bay, $T = 4L(gh)^{-1/2}$, which for a length scale $L \approx 14$ km and a mean depth $h \approx 250$ m, is about 18 min, present in the results as the corresponding spectral peak.

[26] Apart from the last consideration, the results obtained confirm the presence of short-period waves on the free surface in Algeciras Bay, originated in the Strait of Gibraltar and propagated within the bay.

4. Concluding Remarks

[27] Although, to date, there have been no previous studies analyzing the dynamic characteristics of Algeciras Bay, there is a large body of work dealing with the hydrodynamic characteristics of the Strait of Gibraltar. One of the principal aspects reported is the presence of internal waves, which have been extensively studied. However, to date, the disintegration of the principal bore into trains of internal waves of realistic wavelengths had not been reproduced in 3-D numerical models. In this study, we have applied a 3-D numerical model that reproduces the generation of internal bores, the generation of wave trains, and the manifestation

of these trains on the sea surface in the Strait of Gibraltar and Algeciras Bay on the basis of the hydrodynamic characteristics for the principal semidiurnal tidal constituent M_2. The model demonstrates that fronts of wave trains, which move along the strait toward the Mediterranean Sea, are propagated to the interior of Algeciras Bay and are clearly manifested in the free-surface elevation. These results are consistent with the available observational data: both images from space and the experimental series of elevation data recorded in the interior of Algeciras Bay, obtained by pressure sensors. The calculated data reflect similar amplitudes of the short-period waves occurring in the interior of the bay when the observed tidal amplitude is equivalent to that of the M_2 constituent. The experimental results themselves highlight the presence of wave trains in the interior of Algeciras Bay, and their manifestation at the monitoring points occurs at characteristic times prior to the high tide. This behavior coincides with the results predicted by the model, and is described by the results. Therefore, the similarity in the spatial distribution of short-period waves between those generated by the model and those observed in the satellite images and tidal observational data suggests that the model reproduces the breakup of the principal wave, the velocity of propagation, and the wavelength and periods of these fronts moving along the strait, from their generation at the Camarinal Sill to their arrival at points inside the bay. However, as with all models, there are limitations to the results provided by this one. The results from the modeling show that the baroclinic, free-surface approximation in the representation of the pressure included in the momentum equations may be sufficient to reproduce a wide range of the principal nonlinear characteristics of this wave generation, when the spatial grid resolution is fine enough. Nevertheless, it should be noted that the model does not contemplate the additional dispersive contribution of the nonhydrostatic terms, as described by *Morozov et al.* [2002], *Vázquez et al.* [2006], and *Vlasenko et al.* [2009], and hence quantitative differences between observed and predicted data could be reduced when such contribution is considered.

[28] However, the observational data show a wide variability in the amplitudes of these oscillations in function of the phase related to the spring/neap tide cycles of the wave, in consonance with the findings of *Izquierdo et al.* [2001]. Although the numerical results show a good quantitative agreement in the amplitude of the short-period waves when the amplitude of the tidal wave is equivalent to the M_2, the model does not reproduce the variable intensity of the observed wave trains associated with the spring/neap tidal cycle, because it considers only the semidiurnal M_2 constituent. However, using these results, it has been possible to demonstrate that wave-induced sea surface displacement may be used in the context of internal wave studies since such sea surface oscillations can be captured, with sufficient precision, by modern bottom pressure sensors, at least when the internal wave amplitudes are as large as those found in the area of the Strait of Gibraltar and Algeciras Bay. It is also less costly to use this parameter than the expensive mooring lines used in conventional studies, and this methodology may allow researchers to obtain longer simultaneous records of the internal wave events at many points within the area of interest.

[29] **Acknowledgments.** This study was partially supported by Andalusian Government project P06-RNM-01443; the Spanish Ministry of Education and Science projects CTM2007-60408/MAR, CTM2010-20945/MAR, and CTM2008-06421/MAR; and the European Regional Development Fund. A. Izquierdo was funded by EU Marie Curie Fellowship Grant 237426. The SAR images shown in this work were requested from the ESA in the framework of projects ENVISAT-CAT1-P1315 and ENVISAT-CAT1-3473. The ISS009-E-9952 and ISS009-E-9954 images are courtesy of the Image Science and Analysis Laboratory, Johnson Space Center, NASA (http://eol.jsc.nasa.gov). The authors are also sincerely grateful to two anonymous reviewers for their valuable suggestions that have improved this paper.

References

Álvarez, O., A. Izquierdo, B. Tejedor, R. Mañanes, L. Tejedor, and B. A. Kagan (1999), The influence of sediment load on tidal dynamics, a case study: Cadiz Bay, *Estuarine Coastal Shelf Sci.*, *48*, 439–450, doi:10.1006/ecss.1998.0432.

Armi, L., and D. M. Farmer (1988), The flow of Mediterranean water through the Strait of Gibraltar, *Prog. Oceanogr.*, *21*, 1–105, doi:10.1016/0079-6611(88)90055-9.

Bruno, M., R. Mañanes, J. J. Alonso, A. Izquierdo, L. Tejedor, and B. A. Kagan (2000), Vertical structure of the semidiurnal tidal currents at Camarinal Sill, the strait of Gibraltar, *Oceanol. Acta*, *23*, 15–24, doi:10.1016/S0399-1784(00)00104-3.

Bruno, M., J. J. Alonso, A. Cózar, J. Vidal, A. Ruiz-Cañavate, F. Echevarría, and J. Ruiz (2002), The Bowling-water phenomena at Camarinal Sill, the Strait of Gibraltar, *Deep Sea Res., Part II*, *49*, 4097–4113, doi:10.1016/S0967-0645(02)00144-3.

Candela, J. (1990), The barotropic tide in the Strait of Gibraltar, in *The Physical Oceanography of Sea Straits*, edited by L. J. Pratt, pp. 457–475, Kluwer, Dordrecht, Netherlands.

Candela, J., C. Winant, and A. Ruiz (1990), Tides in the Strait of Gibraltar, *J. Geophys. Res.*, *95*, 7313–7335, doi:10.1029/JC095iC05p07313.

De Buen, R. (1924), Avance al estudio de la oceanografía de la Bahía de Algeciras, *Bol. Pescas*, *9*, 1–32.

Flather, R. A., and N. S. Heaps (1975), Tidal computations for Morecambe Bay, *Geophys. J. R. Astron. Soc.*, *42*, 489–517.

Foreman, M. G. G., and R. F. Henry (1989), The harmonic analysis of tidal model time series, *Adv. Water Resour.*, *12*, 109–120, doi:10.1016/0309-1708(89)90017-1.

García, M. J., and J. Molinero (2006), *Estación Mareográfica de Tarifa*, Inst. Esp. de Oceanogr., Madrid. (Available at www.ieo.es/indamar/mareas/documentos/informe-estadisticas-tarifa.pdf.)

García-Lafuente, J. M. (1986), Variabilidad del nivel del mar en el Estrecho de Gibraltar: Mareas y oscilaciones residuals, Ph.D. thesis, Inst. Esp. de Oceanogr., Fuengirola, Spain.

Gerkema, T. (1994), Nonlinear dispersive internal tide: Generation models for a rotating ocean, Ph.D. thesis, Univ. of Utrecht, Utrecht, Netherlands.

Global Ocean Associates (2002), *An Atlas of Oceanic Internal Solitary Waves*, Alexandria, Va. [Available at www.internalwaveatlas.com.]

Godin, G. (1972), *The Analysis of Tides*, Univ. of Toronto Press, Toronto, Ont., Canada.

Izquierdo, A., L. Tejedor, D. V. Sein, O. Backhaus, P. Brandt, A. Rubino, and B. A. Kagan (2001), Control variability and internal bore evolution in the Strait of Gibraltar: A 2-D two-layer model study, *Estuarine Coastal Shelf Sci.*, *53*, 637–651, doi:10.1006/ecss.2000.0706.

Mañanes, R., M. Bruno, J. J. Alonso, B. Fraguela, and L. Tejedor (1998), Non-linear interaction between tidal and subinertial flows in the Strait of Gibraltar, *Oceanol. Acta*, *21*, 33–46.

Marchuk, G. I. (1980), *Methods of Computational Mathematics*, Nauka, Moscow.

Mellor, G. L. (1996), *Users Guide for a Three-Dimensional, Primitive Equation, Numerical Ocean Model*, Program in Atmos. and Ocean Sci., Princeton Univ., Princeton, N. J. [Available at http://jes.apl.washington.edu/modsims_two/usersguide0604.pdf.]

Mellor, G. L., and T. Yamada (1982), Development of a turbulence closure model for geophysical fluid problems, *Rev. Geophys.*, *20*, 851–875, doi:10.1029/RG020i004p00851.

Morozov, E. G., K. Trulsen, M. G. Velarde, and V. I. Vlasenko (2002), Internal tides in the Strait of Gibraltar, *J. Phys. Oceanogr.*, *32*, 3193–3206, doi:10.1175/1520-0485(2002)032<3193:ITITSO>2.0.CO;2.

Orlanski, I. (1976), A simple boundary condition for unbounded hyperbolic flows, *J. Comput. Phys.*, *21*, 251–269, doi:10.1016/0021-9991(76)90023-1.

Pairaud, I. L., F. Lyard, F. Auclair, T. Letellier, and P. Marsaleix (2008), Dynamics of the semi-diurnal and quarter-diurnal internal tides in the Bay of Biscay: Part 1. Barotropic tides, *Cont. Shelf Res.*, *28*, 1294–1315, doi:10.1016/j.csr.2008.03.004.

Parrilla, G., S. Neuer, P. Y. Le Traon, and E. Fernández (2002), Topical studies in oceanography: Canary Islands Azores Gibraltar Observations (CANIGO), vol. 2, Studies of the Azores and Gibraltar regions, *Deep Sea Res., Part II*, *49*, 3951–3955, doi:10.1016/S0967-0645(02)00136-4.

Peaceman, D. W., and H. H. Rachford (1955), The numerical solution of parabolic and elliptic differential equations, *J. Soc. Ind. Appl. Math.*, *3*, 28–41, doi:10.1137/0103003.

Richtmyer, R. D., and K. W. Morton (1967), *Difference Methods for Initial-Value Problems*, Interscience, New York.

Sánchez, P., and J. R. Pascual (1989), Primeras experiencias en la modelación del Estrecho de Gibraltar, in *Seminario Sobre la Oceanografía Física del Estrecho de Gibraltar*, edited by J. L. Almazán et al., pp. 251–282, SECEG, Madrid.

Sánchez Garrido, J. C., J. García Lafuente, F. Criado Aldeanueva, A. Baquerizo, and G. Sannino (2008), Time-spatial variability observed in velocity of propagation of the internal bore in the Strait of Gibraltar, *J. Geophys. Res.*, *113*, C07034, doi:10.1029/2007JC004624.

Sánchez-Román, A., F. Criado-Aldeanueva, J. García-Lafuente, and J. C. Sánchez (2008), Vertical structure of tidal currents over Espartel and Camarinal sills, Strait of Gibraltar, *J. Mar. Syst.*, *74*, 120–133, doi:10.1016/j.jmarsys.2007.11.007.

Sannino, G., A. Carillo, and V. Artale (2007), Three-layer view of transports and hydraulics in the strait of Gibraltar: A three-dimensional model study, *J. Geophys. Res.*, *112*, C03010, doi:10.1029/2006JC003717.

Tejedor, L., A. Izquierdo, D. V. Sein, and B. A. Kagan (1998), Tides and tidal energetics of the Strait of Gibraltar: A modelling approach, *Tectonophysics*, *294*, 333–347, doi:10.1016/S0040-1951(98)00110-3.

Tejedor, L., A. Izquierdo, and D. V. Sein (1999), Simulation of the semidiurnal tides in the Strait of Gibraltar, *J. Geophys. Res.*, *104*, 13,541–13,557, doi:10.1029/1998JC900102.

Tsimplis, M. (2000), Vertical structure of tidal currents over the Camarinal Sill at the Strait of Gibraltar, *J. Geophys. Res.*, *105*, 19,709–19,728, doi:10.1029/2000JC900066.

Tsimplis, M., R. Proctor, and R. Flather (1995), A two-dimensional tidal model for the Mediterranean Sea, *J. Geophys. Res.*, *100*, 16,223–16,239, doi:10.1029/95JC01671.

Vázquez, A., N. Stashchuk, V. Vlasenko, M. Bruno, A. Izquierdo, and P. C. Gallacher (2006), Evidence of multimodal structure of the baroclinic tide in the Strait of Gibraltar, *Geophys. Res. Lett.*, *33*, L17605, doi:10.1029/2006GL026806.

Vázquez, A., M. Bruno, A. Izquierdo, D. Macías, and A. Ruiz-Cañavate (2008), Meteorologically forced subinertial flows and internal wave generation at the main sill of the Strait of Gibraltar, *Deep Sea Res., Part I*, *55*, 1277–1283, doi:10.1016/j.dsr.2008.05.008.

Vlasenko, V., J. C. Sánchez Garrido, N. Stashchuk, J. García-Lafuente, and M. Losada (2009), Three-dimensional evolution of large-amplitude internal waves in the Strait of Gibraltar, *J. Phys. Oceanogr.*, *39*, 2230–2246, doi:10.1175/2009JPO4007.1.

Wang, D. P. (1993), The strait of Gibraltar model: Internal tide, diurnal inequality and fortnightly modulation, *Deep Sea Res., Part I*, *40*, 1187–1203, doi:10.1016/0967-0637(93)90133-N.

Watson, G., and L. S. Robinson (1990), A study of internal wave propagation in the Strait of Gibraltar using shore-based marine radar images, *J. Phys. Oceanogr.*, *20*, 374–395, doi:10.1175/1520-0485(1990)020<0374:ASOIWP>2.0.CO;2.

Watson, G., and L. S. Robinson (1991), A numerical model of internal wave refraction in the Strait of Gibraltar, *J. Phys. Oceanogr.*, *21*, 185–204, doi:10.1175/1520-0485(1991)021<0185:ANMOIW>2.0.CO;2.

Ó. Álvarez, M. Bruno, M. Forero, J. Gómez-Enri, C. J. González, L. López, and R. Mañanes, Department of Applied Physics, University of Cadiz, Campus Universitario de Puerto Real, E-11510 Puerto Real, Spain. (oscar.alvarez@uca.es; miguel.bruno@uca.es; manolo.forerofernandez@alum.uca.es; jesus.gomez@uca.es; carlosjose.gonzalez@uca.es; laura.lopez@uca.es; rafael.salinas@uca.es)

A. Izquierdo, Department of Ocean in the Earth System, Max Planck Institute for Meteorology, Bundestrasse 53, D-20146 Hamburg, Germany. (alfredo.izquierdo@zmaw.de)